Hearing Research 356 (2017) 63–73

Contents lists available at ScienceDirect

Hearing Research

journal homepage: www.elsevier.com/locate/heares

Research Paper

The absence of resting-state high-gamma cross-frequency coupling in patients with tinnitus

Min-Hee Ahn [a], Sung Kwang Hong [a, b], Byoung-Kyong Min [a, *]

[a] Department of Brain and Cognitive Engineering, Korea University, Seoul 02841, South Korea
[b] Department of Otolaryngology, Hallym University College of Medicine, Anyang 14068, South Korea

ARTICLE INFO

Article history:
Received 24 January 2017
Received in revised form
17 October 2017
Accepted 23 October 2017
Available online 31 October 2017

Keywords:
Causality
Cross-frequency coupling
Electroencephalogram
Phase-amplitude coupling
Resting state
Tinnitus

ABSTRACT

Tinnitus is a psychoacoustic phantom perception of currently unknown neuropathology. Despite a growing number of post-stimulus tinnitus studies, uncertainty still exists regarding the neural signature of tinnitus in the resting-state brain. In the present study, we used high-gamma cross-frequency coupling and a Granger causality analysis to evaluate resting-state electroencephalographic (EEG) data in healthy participants and patients with tinnitus. Patients with tinnitus lacked robust frontal delta-phase/central high-gamma-amplitude coupling that was otherwise clearly observed in healthy participants. Since low-frequency phase and high-frequency amplitude coupling reflects inter-regional communication during cognitive processing, and given the absence of frontal modulation in patients with tinnitus, we hypothesized that tinnitus might be related to impaired prefrontal top-down inhibitory control. A Granger causality analysis consistently showed abnormally pronounced functional connectivity of low-frequency activity in patients with tinnitus, possibly reflecting a deficiency in large-scale communication during the resting state. Moreover, different causal neurodynamics were characterized across two subgroups of patients with tinnitus; the T1 group (with higher P300 amplitudes) showed abnormal frontal-to-auditory cortical information flow, whereas the T2 group (with lower P300 amplitudes) exhibited abnormal auditory-to-frontal cortical information control. This dissociation in resting-state low-frequency causal connectivity is consistent with recent post-stimulus observations. Taken together, our findings suggest that maladaptive neuroplasticity or abnormal reorganization occurs in the auditory default mode network of patients with tinnitus. Additionally, our data highlight the utility of resting-state EEG for the quantitative diagnosis of tinnitus symptoms and the further characterization of tinnitus subtypes.

1. Introduction

Tinnitus is the conscious awareness of internally generated sound in the absence of external sound (Jastreboff and Sasaki, 1994; Mohamad et al., 2016) and is usually associated with maladaptive neuroplasticity resultant from deafferentation of the auditory nerve (Faber et al., 2012; Kaya and Elhilali, 2014; Roberts et al., 2013; Schaette and McAlpine, 2011). We recently reported neurophysiological post-stimulus evidence for deficits in both top-down and bottom-up processing in patients with tinnitus (Hong et al., 2016). Yet, it is still debatable whether tinnitus symptoms are also reflected in the resting-state brain (Pierzycki et al., 2016; Schlee et al., 2009a, 2009b). For example, increased spontaneous slow-rhythm activity (e.g., delta and theta activity) is theorized to be associated with deafferented neural activity in patients with tinnitus (Llinas et al., 1999). Conversely, Pierzycki et al. (2016) recently refuted the utility of resting-state whole-scalp electroencephalography (EEG) as a biomarker for tinnitus.

It is noteworthy that previous studies of tinnitus have investigated brain activity in individual frequency bands despite the fact that brain functions (especially those related to perception and cognition) are generally achieved via the synchronization of

Abbreviations: ABR, auditory brainstem response; ACC, anterior cingulate cortex; BA, Brodmann area; CFC, cross-frequency coupling; DLPFC, dorsolateral prefrontal cortex; DTF, directed transfer function; EEG, electroencephalography; EOG, electrooculography; ERP, event-related potential; fMRI, functional magnetic resonance imaging; HL, hearing level; MEG, magnetoencephalography; OAE, otoacoustic emission; PAC, phase-amplitude coupling; PTA, pure tone audiometry; ROI, region of interest; SNR, signal-to-noise ratio; THI, Tinnitus Handicap Inventory; VAS, visual analog scale

* Corresponding author.
E-mail address: min_bk@korea.ac.kr (B.-K. Min).

https://doi.org/10.1016/j.heares.2017.10.008

oscillations across different frequency bands (Cohen, 2008; Schutter and Knyazev, 2012). It has been consistently suggested that synchronization between different cortical areas plays an important role in the pathophysiological basis of tinnitus (Schlee et al., 2008, 2009b). Although some studies (Schlee et al., 2009a; Vanneste et al., 2012) have reported abnormal resting-state cortical coupling in patients with tinnitus using phase-locking analyses, this approach does not provide information about temporal dynamic causal connectivity. Schlee et al. (2009b) analyzed the partial directed coherence of resting-state magnetoencephalography (MEG) data in patients with tinnitus; however, the results did not address cortical coupling across different frequency bands. Thus, uncertainty still exists regarding the neural correlates of tinnitus in the resting-state brain.

Here, we hypothesized that studying the interaction of different oscillatory activities in the tinnitus hub would inform the neural correlates of tinnitus. Interactive relationships between oscillations in different bands can be investigated using a cross-frequency coupling (CFC) analysis (Canolty et al., 2006; Osipova et al., 2008). Moreover, knowledge about cross-frequency interactions of spontaneous brain activity might provide significant insight into the characteristics of the default mode network in patients with tinnitus. Phase-amplitude coupling (PAC; also known as “nested oscillations”) is one type of CFC in brain rhythms (Tort et al., 2010) where the phase of the lower frequency oscillation drives the power of the coupled higher frequency oscillation, resulting in synchronization of the amplitude envelopes of faster rhythms with the phases of slower rhythms (Fig. 1). Measures of cross-frequency PAC can therefore indicate the relationship between activities correlated with low-frequency oscillations (e.g., sensory inputs) and local cortical activities (e.g., local computations) that modulate the amplitudes of higher frequency oscillations (Canolty and Knight, 2010).

PAC is affected by behavioral tasks (Voytek et al., 2010) and is potentially related to attentional selection, sensory integration, and memory processing (Lisman, 2005; Lisman and Idiart, 1995; Schroeder and Lakatos, 2009). Although Adamchic et al. (2014) observed abnormal CFC in the tinnitus network, frequencies in this study were confined below 50 Hz; indeed, Canolty and Knight (2010) and Canolty et al. (2006) reported that high-gamma (>50 Hz) CFC was critical for understanding effective local computations as well as large-scale inter-regional communication during cognitive processing in humans. Therefore, in the present study, we investigated CFC, including high-gamma activity, and compared the Granger causal connectivity between healthy control subjects and patients with tinnitus in the resting state. We additionally examined whether there were differences in PAC between two patient subgroups (i.e., T1 and T2; see our recent study, Hong et al., 2016).

2. Materials and methods

2.1. Participants

This study analyzed resting-state EEG data sampled from participants in a previous study by our group (Hong et al., 2016). Based on a subject debriefing that we conducted after the resting-state EEG acquisition, we excluded five patients with tinnitus who reported experiencing sleepiness during the resting-state evaluation. To compensate for the loss of subjects and to enhance the statistical power, we recruited 12 new subjects (six patients with tinnitus and six healthy control subjects) for inclusion in the present study. Accordingly, we analyzed the EEG data recorded from 16 patients with tinnitus (eight women; mean age, 28.9 years) and 16 age/sex-matched healthy volunteers (eight women; mean age, 27.4 years). Data were collected in accordance with the ethical guidelines of the Institutional Review Board of Hallym University College of Medicine and the Declaration of Helsinki (World Medical Association, 2013). All patients showed signs of definitive tinnitus for at least 3 months but less than 1 year, and had normal hearing on conventional hearing tests (Table 1). Normal hearing was defined as follows: (1) a pure tone audiometric (PTA) threshold of 25 dB hearing level (HL) or better for all octave frequencies from 250 to 8000 Hz; (2) transient evoked otoacoustic emission (OAE) with a signal-to-noise ratio (SNR) > 5 dB and a distortion product OAE with an SNR > 3 dB on OAE tests; (3) a waves I–III inter-peak latency < 2.4 ms and a wave V latency < 6.2 ms on 90 dB nHL click-evoked auditory brainstem response (ABR) tests; and (4) a normal tympanic membrane on otoscopy. It is possible that peripheral damage was present in some patients, but was not detectible by routine audiometry (Adjamian et al., 2012). For example, some patients with high-frequency tinnitus may have cochlear deafferentation despite exhibiting audiometrically normal thresholds (Weisz et al., 2006). Additionally, the recovery of audiometric thresholds to normal levels after temporary hearing loss does not indicate the reversal of damage to inner ear structures (Kujawa and Liberman, 2009). It has also been suggested that individuals with tinnitus who show apparently normal audiograms can have “hidden hearing loss” defined as damage to the auditory nerve fibers (Schaette and McAlpine, 2011). Despite these possibilities, all patients with tinnitus in the present study exhibited normal latencies in waves I–III of the ABRs and normal OAEs, which usually indicate the integrity of the peripheral auditory nerves (Moller et al., 1981; Moller and Jannetta, 1982) and normal function of the cochlear hair cells (Kemp, 1978; Mills and Rubel, 1994), respectively. Thus, “normal hearing” in this study was defined as a normal hearing ability in the frequency range of 250–8000 Hz on conventional tests (e.g., PTA, OAE, ABR, and otoscopic

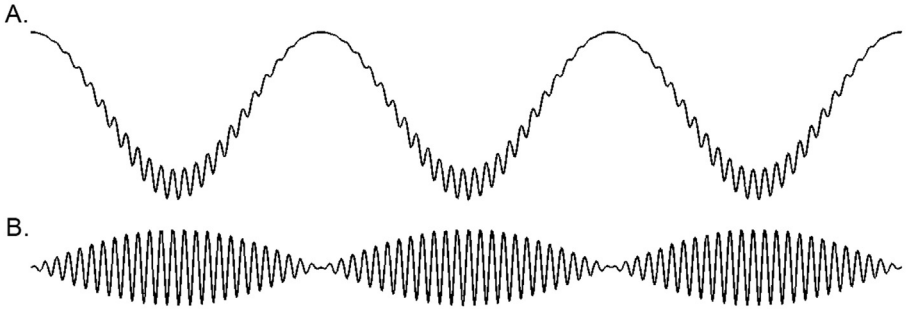

Fig. 1. A schematic sample of low-frequency phase/high-frequency amplitude coupled modulation. (A) The sum of fast and slow oscillations, where the amplitude of the fast oscillation's envelope changes with the phase of the slower oscillation. (B) The fast oscillation and variation in its amplitude only. Note that the fast rhythm's amplitude reaches a maximum when the slower oscillation is at a specific phase, the so-called coupling phase.

Table 1
Characteristics of the tinnitus group.

ID	Subgroup	Sex	Age (years)	Tinnitus frequency (kHz)	Deficit side	Etiology	Right[a] (dB HL)	Left[a] (dB HL)
1	T2	F	22	8	Left	Idiopathic	−2	2
2	T1	F	30	8	Right	Idiopathic	5	5
3	T2	F	35	8	Both	Idiopathic	10	9
4	T1	M	26	8	Left	Idiopathic	0	−1
5	T2	M	26	8	Left	Idiopathic	2	1
6	T1	M	17	8	Left	Idiopathic	5	6
7	T1	M	35	8	Left	Idiopathic	4	2
8	T2	F	40	0.25	Both	Idiopathic	9	11
9	T1	F	41	8	Left	Idiopathic	0	0
10	T2	M	41	0.125	Right	Idiopathic	9	8
11	T1	M	24	8	Left	Idiopathic	9	13
12	T1	M	23	4	Right	Idiopathic	10	10
13	T2	F	24	4	Both	Idiopathic	9	−1
14	T1	M	22	4	Left	Idiopathic	4	10
15	T2	F	37	8	Right	Idiopathic	5	5
16	T2	F	20	4	Left	Idiopathic	8	13

[a] Pure tone audiometric (PTA) threshold. HL, hearing level; F, female; M, male.

examinations), but not necessarily the absence of deafferentation.

To reduce the possibility of including patients with hidden hearing loss and to ensure comparable cognitive ability between patients and healthy volunteers, we did not include subjects who (1) were older than 50 years of age; (2) had a current or previous history of vertigo, Meniere's disease, noise exposure, hyperacusis, or psychiatric problems; (3) were exposed to ototoxic drugs; or (4) had complex or poorly defined tinnitus (e.g., failure of tinnitus pitch matching). Additionally, all patients completed a tinnitus questionnaire, which included a 0–10 visual analog scale (VAS), to evaluate each patient's level of annoyance from tinnitus (where 0 indicated not annoying and 10 indicated extremely annoying) and a Korean version of the Tinnitus Handicap Inventory (THI) questionnaire that was translated from the original THI of the American Tinnitus Association (Newman et al., 1996). The control group included healthy participants who did not show signs of tinnitus or cochlear damage as assessed by the PTA, OAE, and ABR tests. The control group was considered to be otolaryngologically normal. The audiometric evaluations and tinnitus tests that were performed in both groups have been previously described (Hong et al., 2016).

2.2. Experimental design and EEG acquisition

We recorded the EEG signals during the resting state for 5 min from all participants. Although an evaluation window of 5 min has limited utility for investigating the resting state, it has been reported that global connectional properties in the brain stabilize with acquisition times as brief as 5 min (Van Dijk et al., 2010). During the resting state, participants were seated in a soundproof room and instructed to fix their eyes on a fixation cross presented on a monitor within a visual angle of 1.2° at a distance of 80 cm. After acquiring the EEG data during the resting state, a subject debriefing was conducted to determine whether any of the subjects was sleepy during the resting state. A BrainAmp DC amplifier (Brain Products, Germany) with a 32 Ag/AgCl-electrode actiCAP was used to measure the EEG signals. Electrodes were positioned in accordance with the international 10–10 system; a reference electrode was placed on the tip of the nose and the AFz electrode was used as a ground. Electrode impedances were maintained below 5 kΩ prior to recording. The EEG signals were recorded at 1000 Hz (analog high-pass filter with a cutoff frequency of 0.5 Hz, and notch filter at 60 Hz to reduce the power-line artifact). Eye movement activity was monitored using an electrooculography (EOG) electrode placed below the left eye, and vertical and horizontal electro-ocular activities were computed using two pairs of electrodes placed vertically and horizontally with respect to both eyes (i.e., Fp1 and EOG for vertical EOG; F7 and F8 for horizontal EOG). Any EOG and muscle artifacts were corrected offline using an independent component analysis (ICA) (Makeig et al., 1997; Muthukumaraswamy, 2013). This method was employed to minimize any possible high-frequency frontalis and temporalis muscle artifacts (Klem, 2003).

2.3. Cross-frequency coupling analysis

In order to investigate CFC, we computed the coherence between the low-frequency (1–13 Hz; less than the beta band) signal and the time-course of power at higher frequencies (up to 250 Hz). Coherency $Coh(f_1,f_2)$ was estimated between the signal X_t and the estimated time course of power $P_t(f_2)$ for a given frequency f_1 by applying a sliding Hanning tapered time window followed by a Fourier transformation. We applied a Hanning taper to an adaptive time window of 6 cycles for each frequency ($\Delta T = 6/f$). Coherency was calculated with respect to the two time series as shown in the following equation:

$$\mathrm{Coh}(f_1,f_2) = \frac{\sum_{k=1}^{M} \tilde{X}^k(f_1)\,\tilde{P}^{*k}(f_1,f_2)}{\sqrt{\sum_{k=1}^{M}\left|\tilde{X}^k(f_1)\right|^2 \sum_{k=1}^{M}\left|\tilde{P}^k(f_1,f_2)\right|^2}}$$

where

$$\tilde{X}^k(f_1) = \Delta t \sum_{l=1}^{M} h_l X_{L\left(k-\frac{1}{2}\right)+l}\, e^{-i2\pi f_1 l \Delta t}$$

$$\tilde{P}^k(f_1,\ f_2) = \Delta t \sum_{l=1}^{M} h_l P_{L\left(k-\frac{1}{2}\right)+l}(f_2) e^{-i2\pi f_1 l \Delta t}$$

Hence, $\Delta t = 1/F_s$, where F_s is the sampling frequency. The length of the time window decreased with frequency: $K = F_s M/f_2$, where M is the number of cycles per time window. Coherency was computed with respect to the two time series divided into M segments that were each 2048 data points in length (L) (Osipova et al., 2008). Coherence was the absolute value of coherency $|Coh(f_1,f_2)|$. In this case, h_l in the above equation set refers to a 2048-point Hanning window and * refers to the complex conjugate. This allowed us to perform a sensor-by-sensor characterization of phase-to-power cross-frequency interactions with respect to f_1 and f_2.

To compute spectrograms of EEG activity averaged at low-frequency phase troughs with the highest PAC, signals were first filtered in the delta band using a narrow band-pass filter (a symmetrical finite impulse response filter [~35 dB/octave roll-off] with a specific nesting frequency within the delta frequency range [1–4 Hz]), and then amplitude troughs were identified from the filtered signals. For each marked trough, a time window from −0.5 to 0.5 s was extracted and a time-frequency decomposition was performed to obtain the power of all averaged time-frequency plots (Fig. 2B) using Brainstorm software (Tadel et al., 2011). The PAC analysis was conducted on the 60-Hz notch-filtered EEG data.

Given that (1) dipole-sources for auditory processing generate the most prominent activity around the vertex of the brain (i.e., the location of the Cz electrode; Näätänen et al., 1992); (2) short-latency auditory evoked potential components are typically recorded between the Cz electrode and both earlobes (Legatt, 2011); and (3) the Fz area is considered to be a representative position for prefrontal top-down processing (Keeser et al., 2011; Min and Park, 2010), we examined Fz-phase/Cz-amplitude and Cz-phase/Fz-amplitude CFC. Delta (1–4 Hz) phase and high-gamma (50–250 Hz) amplitude cross-frequency modulation was investigated based on previous reports indicating that the amplitude of high-gamma oscillations is modulated by the phase of lower frequency oscillations (Buzsaki and Draguhn, 2004; Canolty et al., 2006; Lakatos et al., 2005). The maximum PAC values within these frequency ranges were compared using independent-sample Mann-Whitney *U* tests (for a between-subjects design) and Wilcoxon tests (for a within-subject design). All analyses were performed using MATLAB (ver. R2016a, MathWorks, Natick, MA) or SPSS Statistics (ver. 22, IBM, Armonk, NY). In order to further investigate the characteristic neurophysiological alterations in patients with tinnitus, *post hoc* tests were performed according to the tinnitus subgroup (i.e., T1 and T2), which was assigned using a median split based on P300 amplitudes (threshold, 11.237 μV; the T1 group had higher P300 amplitudes while the T2 group had lower P300 amplitudes) during the processing of target stimuli in the oddball task of our previous study (Hong et al., 2016). This distinction was made based on the hypothesis that the P300 component reflects fundamental cognitive processes (Donchin and Coles, 1988; Johnson, 1988; Picton, 1992; Polich, 1993).

2.4. Granger causality analysis

Granger causality (Granger, 1969) analyses allow for the noninvasive assessment of brain network connectivity (Astolfi et al., 2004; Babiloni et al., 2005; Ding et al., 2007). The far-field nature of noninvasive EEG recording complicates the estimation of causal interactions with challenges such as the source leakage effect. In the present study, we addressed source leakage using an innovative approach combining electrophysiological source imaging with a Granger causality analysis, which has demonstrated promising utility for the noninvasive identification of brain network connectivity (Astolfi et al., 2004; Babiloni et al., 2005; Ding et al., 2007). The eConnectome software (He et al., 2011) offers a solution to reduce source leakage by reconstructing source signals in the brain that underlie sensor signals. Phase scrambling is a procedure used to assess the statistical significance of arbitrary connectivity values calculated based on autoregressive modeling. Using the scrambling process, the calculated original connectivity values are compared to a population of bootstrapped values under a null hypothesis of no effective connectivity. However, the significance level determined by phase scrambling is not necessarily related to source leakage; scrambling may not be sufficient to fundamentally resolve apparent connectivity induced by source leakage. In the eConnectome software, we used an approach estimating cortical source signals with a subsequent assessment of

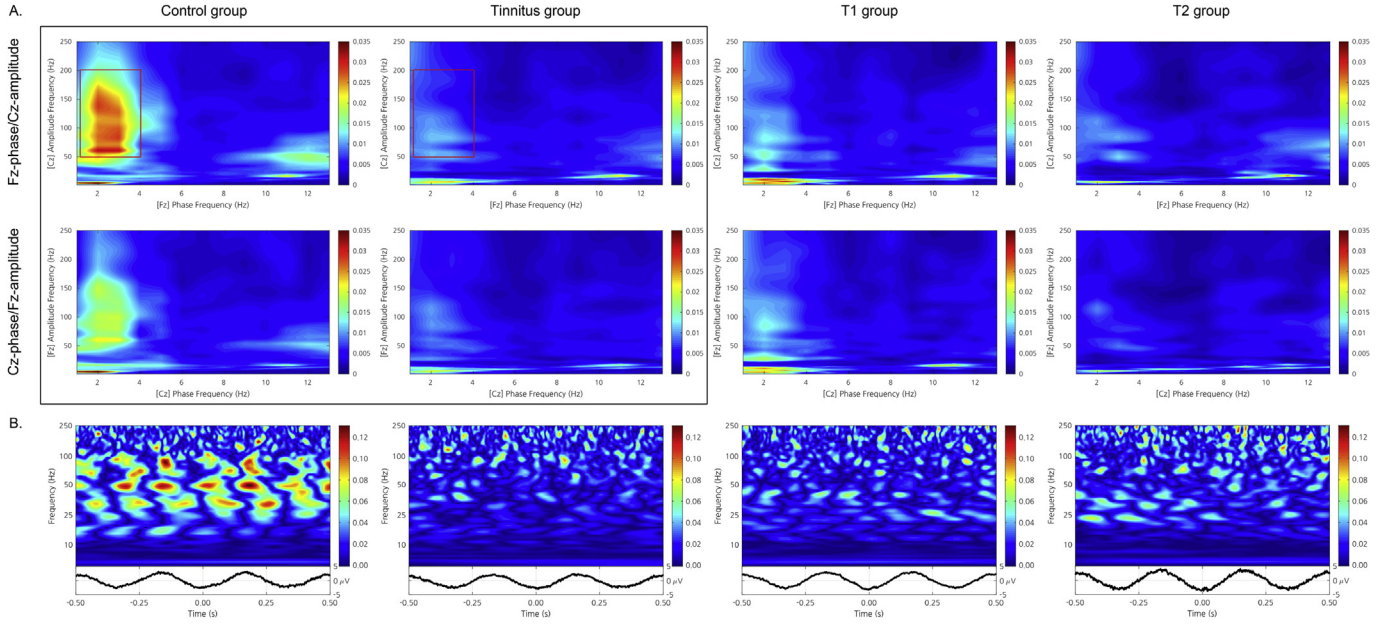

Fig. 2. Resting-state grand-averaged cross-frequency phase-amplitude couplings in healthy participants, patients with tinnitus, and the T1 and T2 subgroups (from left to right). (A) Phase-amplitude coupling as a function of analytic amplitude (1–250 Hz) and analytic phase (1–13 Hz) for the Fz-phase/Cz-amplitude (upper row) and the Cz-phase/Fz-amplitude (lower row) combinations. Note the obvious absence of delta-phase (Fz)/high-gamma-amplitude (Cz) coupling in the tinnitus group compared to the control group (areas highlighted in red). The color bar indicates coherence (ranging from 0 to 1), with 0 representing perfect non-coherence and 1 indicating 100% coherence. Larger values indicate stronger cross-frequency modulation. (B) Individual samples of phase-locked modulation of power in EEG signals from the Cz electrode. Upper panels: Time-frequency plots of mean power modulation time-locked to the delta trough (3 Hz). Red and blue indicate power increases and decreases relative to the mean power, respectively. The scale bar indicates the unitless normalized Z-scores. Lower panels: Delta trough-locked averages of low-frequency (3 Hz) time series. Note that high-gamma power was coupled with the delta phase in the control group but not in the tinnitus group.

connectivity patterns in the source domain. This de-convoluted inverse solution is expected to have less mixing as compared with scalp EEG signals. As such, this method has adopted the concept of regions of interest (ROIs) to image functional connectivity among cortical regions. This ROI-based approach further reduces the effects of signal mixing, as less mixing is anticipated when signals are derived from non-adjacent locations (He et al., 2011). Therefore, functional causal connectivity in the resting state was mapped for each group using the eConnectome software (Dai and He, 2011; Dai et al., 2012; He et al., 2011), which enabled cortical source imaging and a subsequent connectivity analysis of cortical source activity. Granger causality was investigated using grand-averaged oscillatory activity in the following frequency bands: delta (1–4 Hz), theta (4–8 Hz), alpha (8–13 Hz), beta (13–30 Hz), low gamma (30–50 Hz), and high gamma (50–250 Hz).

In the eConnectome software (He et al., 2011), the cortical current density source model (Dale and Sereno, 1993) was used to solve the inverse problem from scalp EEG to cortical source distribution using a minimum norm estimate or lead-field weighted minimum norm algorithm with the aid of the boundary element method (He et al., 1987). Using the Montreal Neurological Institute template, the scalp, skull, and brain surfaces were segmented and reconstructed. The scalp surface consisted of 2054 triangles and formed the sensor space. Such generic realistic head models have been suggested to improve source analysis accuracy (Darvas et al., 2006; Valdes-Hernandez et al., 2009). The ROI source was then computed by averaging the estimated cortical sources in the ROI. Cortical ROI functional connectivity was computed using the directed transfer function (DTF) method in selected frequency components among selected ROIs. The DTF method was developed to describe causality among an arbitrary number of signals (Astolfi et al., 2007; Babiloni et al., 2005). Based on the most pronounced post-stimulus cortical activity observed in our previous study (Hong et al., 2016), 16 bilateral ROIs were selected (Brodmann areas [BAs] 24L/R, 27L/R, 32L/R, 39L/R, 40L/R, 41L/R, 42L/R, and 46L/R) to map directional connectivity. These cortical areas play significant roles in auditory processing. BA 24 is the ventral anterior cingulate cortex (ACC) and BA 32 is the dorsal ACC. The ACC is associated with top-down attentional inhibitory regulation (Johnston et al., 2007; Silton et al., 2010) and conflict monitoring (Apps et al., 2012; Borsa et al., 2016; Botvinick et al., 2004). BA 27 is the hippocampus/parahippocampal region and is associated with short-term memory function (Vertes, 2005), navigating the auditory scene (Teki et al., 2012), and auditory-verbal memory function (Fletcher et al., 1995; Squire et al., 1992). BA 39 (the angular gyrus) and BA 40 (the supramarginal gyrus) are parts of Wernicke's area involved in the comprehensive processing of presented auditory stimuli. BA 41 and 42 closely correspond to the primary auditory cortex, which is also involved in the processing of presented auditory stimuli. BA 46 is the part of the dorsolateral prefrontal cortex (DLPFC), which participates in executive cognitive functions such as planning, monitoring, inhibiting, and working memory (Fuster, 2008, 2013; Gazzaley and D'Esposito, 2007). Bonferroni-corrected ($p < 10^{-6}$) causal connectivities across the 16 ROIs are shown in Fig. 3.

The DTF function yields arbitrary values representing functional connectivity, which are still subject to statistical assessments of significance (He et al., 2011). Since the DTF function has a highly nonlinear relationship to the time series data from which it is derived, a non-parametric statistical testing method based on surrogate data is used to evaluate the significance of the estimated connectivity measures (Ding et al., 2007). We transformed the original time series to the Fourier space, preserving the magnitudes of Fourier coefficients but randomly and independently shuffling the phases of Fourier coefficients. Surrogate data in the Fourier space were then transformed back to the time domain. This process of phase shuffling preserves the spectral structure of the time series and is thus suited for DTF analyses, which measure frequency-specific causal interactions. After shuffling, the connectivity estimation was applied to the surrogate data. We repeated the shuffling and connectivity estimation procedure 1000 times for each set of source time series, creating an empirical distribution of DTF values under the null hypothesis of no causal connectivity ($p < 0.05$) (Ding et al., 2007).

3. Results

3.1. Cross-frequency coupling

Healthy participants showed significantly higher PAC values than did patients with tinnitus for both Fz-phase/Cz-amplitude coupling (mean ± standard deviation; 0.0561 ± 0.0413 vs. 0.0194 ± 0.014, respectively; $p < 0.001$; see the boxes highlighted in red in Fig. 2A) and Cz-phase/Fz-amplitude coupling (0.037 ± 0.0379 vs. 0.0152 ± 0.00576, respectively; $p < 0.01$). The Fz-phase/Cz-amplitude coupling was significantly more prominent than was the Cz-phase/Fz-amplitude coupling in the healthy control group (0.0561 ± 0.0413 vs. 0.037 ± 0.0379, respectively; $p < 0.005$). However, there were no significant differences between these two different directional couplings in the tinnitus group. *Post hoc* comparisons revealed that delta-phase/high-gamma-amplitude coupling was not significantly different between the T1 and T2 groups. These two subgroups showed a lack of CFC effects in all directions (Fig. 2). Delta trough-locked averaging of the time-frequency plane in the control group showed obvious coupling between delta-phase and high-frequency power, with an increase or decrease in power relative to baseline depending on the phase of delta activity (Fig. 2B). Delta coupling was broadband from 30 to 200 Hz, with the strongest modulation occurring in the high-gamma band. Notably, these features were not observed in the tinnitus group. The CFC data from individual subjects are provided in Supplementary Table 1.

3.2. Granger causal connectivity

Color-scaled directional arrows link two causally connected ROIs (across the 16 ROIs) only when the Granger causality is statistically significant using a surrogate approach (1000 surrogate data sets, $p < 0.05$; Fig. 3). It is noteworthy that there were abnormally pronounced distributions of low-frequency activity, particularly delta activity, in the tinnitus group compared to the control group. Resting-state Granger causal connectivity was centered on the ACC (BAs 24 and 32) and DLPFC (BA 46) in all frequency bands in both the control and tinnitus groups. Additionally, prominent bidirectional connectivity of low-frequency activity (e.g., delta and theta) between frontal top-down areas and primary auditory bottom-up areas was uniquely observed in the tinnitus group. Subsequent comparisons revealed opposing dissociations of resting-state causal connectivity in the low-frequency bands between the T1 and T2 subgroups. That is, the T2 group exhibited an abnormal dominant influence of the primary auditory cortex (BA 41L) on frontal top-down areas (BA 46L), whereas the T1 group showed dominant influence of a frontal top-down area (BA 32L) on the auditory cortices (BAs 39–42; Fig. 3). The causal-connectivity data from individual subjects are shown in Supplementary Table 2.

4. Discussion

In the present study, healthy participants exhibited clear delta-

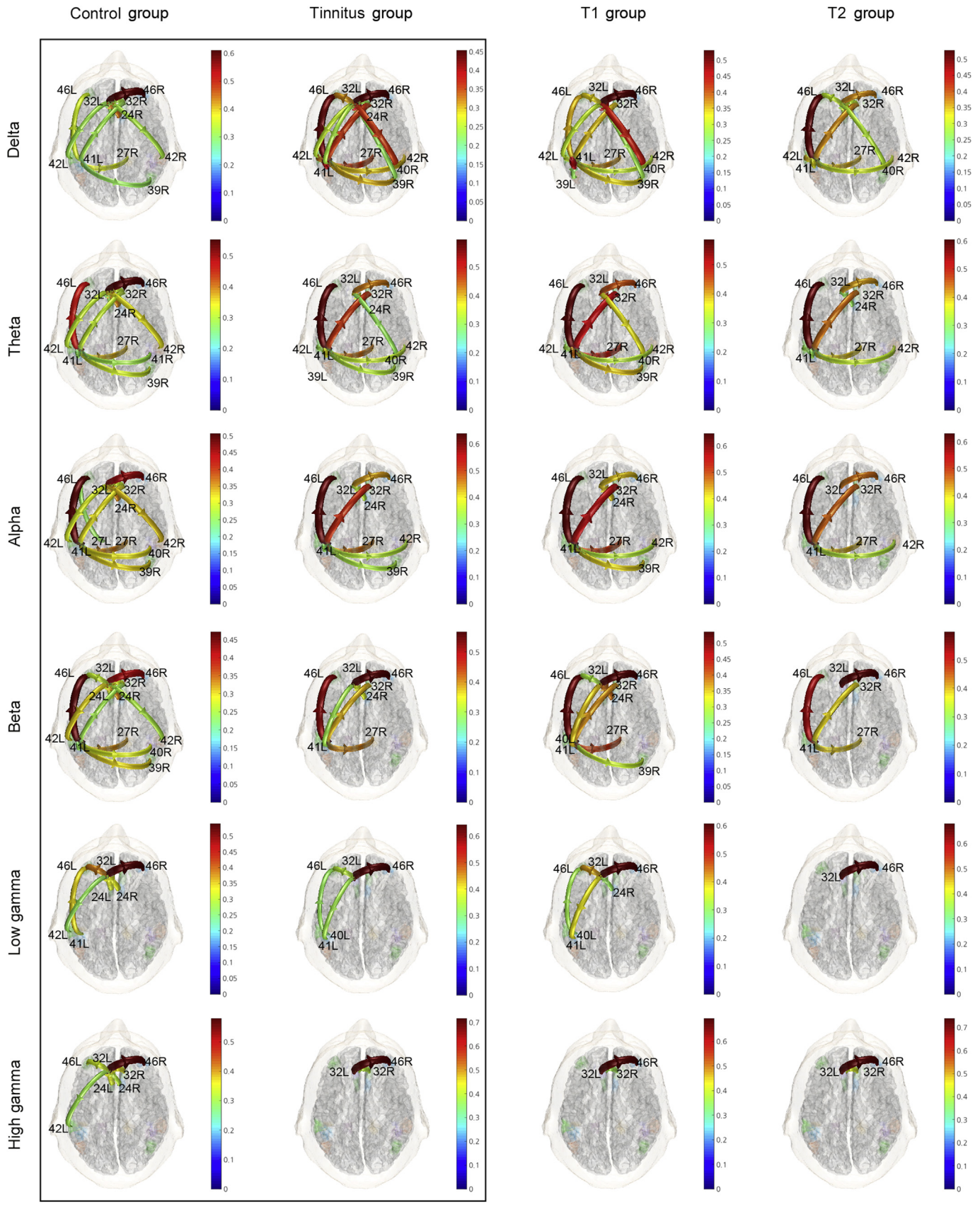

Fig. 3. Resting-state Granger causal connectivity of grand-averaged delta (1–4 Hz), theta (4–8 Hz), alpha (8–13 Hz), beta (13–30 Hz), low-gamma (30–50 Hz), and high-gamma (50–250 Hz) activity in healthy participants, patients with tinnitus, and the T1 and T2 subgroups (from left to right). Color-scaled directional arrows link two causally connected ROIs across the 16 ROIs (Brodmann areas [BAs] 24L/R, 27L/R, 32L/R, 39L/R, 40L/R, 41L/R, 42L/R, and 46L/R) when Granger causality was statistically significant (i.e., $p < 0.05$). The

phase/high-gamma-amplitude coupling from frontal to central brain regions that was notably absent in patients with tinnitus. Coupled low-frequency/high-frequency oscillations may serve as an important mechanism for long-range communication across different brain regions (Schlee et al., 2009a). Indeed, coordinated slow-rhythm activity has been proposed to underlie long-range brain networks, where local information processing occurs via fast-rhythm activity nested into slow-rhythm activity (von Stein and Sarnthein, 2000). Since coherent low-frequency oscillations seem to play an essential role in controlling large-scale networks (Benchenane et al., 2010; Miller, 2013), the absence of delta/high-gamma PAC in the tinnitus group likely reflects a deficiency in the integrated action of inter-regional functional brain networks in the resting state. Consistent with this idea, our Granger causal connectivity analysis identified abnormal inter-regional connectivity in the tinnitus group vs. the control group, particularly in low-frequency oscillations (delta and theta activity). Compared to the control group, low-frequency connectivity in the tinnitus group was characterized by prominently distributed functional connections, which may be indicative of imprudent overregulation throughout the brain and thus inefficient control in the preparatory mental state for upcoming stimulus information processing. Therefore, tinnitus seems to be related to a deficiency in the modulation of high-frequency amplitudes by low-frequency phases, which yields inefficient control in the preparatory mental state before information processing.

It is well known that EEG signals can be contaminated by muscle artifacts in high frequency ranges. Whereas muscle-induced high-frequency artifacts are most prominent at 20–30 Hz frontally and 40–80 Hz temporally (Goncharova et al., 2003), our CFC observations were in the range of 80–250 Hz. Moreover, since EOG and muscle artifacts were corrected offline using an ICA (Makeig et al., 1997; Muthukumaraswamy, 2013), the high-frequency EEG activity we observed in the present study was virtually free from frontalis and temporalis dominant muscle artifacts. Lastly, the delta-phase/high-gamma-amplitude coupling we observed in the present study had directionality (i.e., for the Fz-phase/Cz-amplitude combination, but not for the Cz-phase/Fz-amplitude combination; Fig. 2A). A result driven by high-frequency muscle artifacts contaminating the high-gamma EEG activity would have lacked directionality. Collectively, these findings suggest that the high-gamma activity we observed in the present study was likely not driven by contaminating muscle artifacts.

To the best of our knowledge, this is the first study to identify clear differences in resting-state high-gamma CFC and cross-regional interactions between patients with tinnitus and healthy participants. Currently, it is unclear why this effect has not been demonstrated previously. One potential explanation is that the CFC analysis we employed is state-of-the-art, thus only a few EEG laboratories have analyzed their data using this method. Moreover, the researchers that have used this CFC analysis mainly applied it on data from normal healthy subjects. Indeed, few prior studies have attempted to investigate CFC in the resting state in patients with tinnitus, particularly including high-gamma activity. Adamchic et al. (2014) reported abnormal CFC in the tinnitus network, but frequencies in this study were confined to below 50 Hz. All of the above factors likely explain why the abnormal lack of resting-state high-gamma CFC in tinnitus patients has not been detected previously.

Our observations of cross-frequency interactions and spatio-temporal distributions of spontaneous brain activity may provide psychophysiological insights into the behavior of the tinnitus default mode network. It is known that low-frequency activity can be entrained by rhythmic external sensory or motor events (Luo and Poeppel, 2007; Saleh et al., 2010) as well as by internal cognitive processes such as learning and memory (Rizzuto et al., 2006). Accordingly, the presence of PAC accompanied by low-frequency phase entrainment implies that the modulation of high-frequency amplitudes is coordinated according to slower, behaviorally relevant external and internal stimuli (Canolty and Knight, 2010). In general, biological organisms actively control the temporal targeting of their own sensory experiences (e.g., contrast hearing and listening); thus, the arrival of neuronal spikes carrying stimulus information to early sensory areas will occur in rhythmic volleys, producing intentionally regulated rhythmicity of perception and multisensory integration (Canolty and Knight, 2010). In accordance with this consideration, we observed pronounced periodicity of the amplitude variations for high-gamma oscillations locked to trough phases of the lower (delta) oscillations in healthy participants, but these couplings were absent in patients with tinnitus.

Resting-state Granger causal connectivity was centered on the ACC (BAs 24 and 32), which is associated with top-down attentional inhibitory regulation (Johnston et al., 2007; Silton et al., 2010) and conflict monitoring (Apps et al., 2012; Borsa et al., 2016; Botvinick et al., 2004). In addition, dominant connectivity during the resting state was observed in BA 46 (part of the DLPFC), which is involved in executive cognitive functions such as planning, monitoring, inhibiting, and working memory (Fuster, 2008, 2013; Gazzaley and D'Esposito, 2007). Consistent with previous studies, most symptoms of tinnitus can be observed in tandem with the activation of non-auditory brain structures such as the DLPFC (Schlee et al., 2009b; Vanneste et al., 2010) and ACC (Muhlau et al., 2006; Vanneste et al., 2010). Heeren et al. (2014) also reported that the degree of executive control impairment was correlated with the duration of tinnitus in patients. The abovementioned prefrontal areas are involved in auditory attention (Alain et al., 1998; Lewis et al., 2000; Voisin et al., 2006) and thus the top-down regulation of auditory processing (Mitchell et al., 2005). This is supported by an electrophysiological study suggesting that tinnitus occurs as a result of dysfunctional top-down inhibitory processes (Norena et al., 1999). Hence, the globally distributed delta activity we observed in the tinnitus group likely reflected the abnormal distribution of cognitive resources in the resting state.

Patients in the present study had tinnitus for less than 1 year at the time of testing. It has been reported that, compared to patients with long-term tinnitus (>1 year), patients with recently diagnosed tinnitus (<1 year) exhibit enhanced recruitment of the posterior region of the brain (consistently shown in our observations of resting-state causal connectivity; Fig. 3) and an increased correlation of activity between the default mode network and the precuneus at rest (Carpenter-Thompson et al., 2015). Interactions between top-down and bottom-up processes contribute to the allocation of limited perceptual processing resources to one or more sound-parameter dimensions (Caporello Bluvas and Gentner, 2013). In general, the active redirection of attention embedded in a top-down process precedes an event or stimulus in the resting state; however, the spontaneous activity that occurs in the resting state of patients with tinnitus might produce abnormal top-down modulation (i.e., dysfunction in a specific reallocation of attention), resulting in inefficient perceptual identification in response to directed attention.

numbers of BAs demonstrating pronounced connectivity are marked at their positions on the topography. Color-scaled arrows in the cortical connectivity image represent the degree of causal connectivity (ranging from 0 to 1). The topographical view is from the vertex, with the nose at the top of the image.

In addition to common frontal interconnections (from BA32L to BA46R and BA24R), observed in both the control and patient groups during the resting state, significant abnormal connectivity was detected in the low-frequency bands, particularly delta, in patients with tinnitus during the resting state. Although resting-state CFC was not significantly different between the T1 and T2 groups, the T1 group showed abnormal frontal-to-auditory cortical information flow, whereas the T2 group exhibited abnormal auditory-to-frontal cortical information control. That is, in the T2 group, low-frequency causal connectivity in the resting state was abnormally dominant due to the influence of the primary auditory cortex (BA 41L) on frontal top-down areas (BA 46L; Fig. 3). Alternatively, strong causal connectivity from a frontal top-down area (BA 32L) to the auditory cortices (BAs 39, 40, 41, and 42) was observed in the T1 group. This dissociation between the T1 and T2 groups with regard to the resting-state causal connectivity in the low-frequency band corroborates our recent post-stimulus observations (Hong et al., 2016), in which the T1 group exhibited impairment in bottom-up processing during a passive listening task while the T2 group showed impairment in top-down processing during the active oddball task. From a perspective of resting-state connectivity, bottom-up processing in the auditory cortex may have been abnormally suppressed in the T1 group, while there was abnormal control of frontal top-down areas in the T2 group. Thus, T2-type tinnitus symptoms may be due to maladaptive afferentation of the auditory pathway, whereas T1-type tinnitus symptoms may be due to maladaptive efferentation of the auditory pathway. This hypothesis reinforces the idea that differential top-down impairments exist alongside deficits in bottom-up processing in patients with tinnitus.

Directional delta/high-gamma coupling in healthy participants (i.e., stronger in the Fz-phase/Cz-amplitude CFC, but weaker in the Cz-phase/Fz-amplitude CFC) was suggestive of unidirectional modulation from frontal top-down areas to primary auditory bottom-up areas. The absence of unidirectional frontal-to-central modulation in patients with tinnitus implies that the neural basis of tinnitus involves abnormalities in prefrontal functions. Given that the prefrontal cortex is essential for higher-order cognitive control and goal-directed behaviors (Fuster, 1989; McNamee et al., 2015; Miller and Cummings, 2007), our data suggest that patients with tinnitus suffer some degree of dysfunction in cognitive control during the resting state, consistent with a theory of abnormal top-down modulation, dysfunctional cognitive (or attentional) resource allocation, and impaired perceptual identification. As high gamma (>50 Hz) CFC is important for understanding effective local and inter-regional communication during cognitive processing in humans (Canolty and Knight, 2010; Canolty et al., 2006), the present study provides evidence for the utility of resting-state EEG and CFC as quantitative biomarkers in patients with tinnitus. In addition, since the resting-state connectivity is functionally related to the post-stimulus P3 event-related potential (ERP) component (Li et al., 2015), the abnormal lack of an Fz-Cz resting-state PAC pattern in the tinnitus group suggests the presence of impairments in post-stimulus information processing.

The present study had some limitations. First, although CFC was computed on the scalp level, the Granger causality analysis was performed on the cortical level, and EEG source localization was based on a limited number of scalp channels. In general, the accuracy of EEG source localization relies on sufficient spatial frequency in the scalp potential field (Song et al., 2015; Srinivasan et al., 1998). Although data collection from more than 32 channels typically guarantees confidence for source localization (Lantz et al., 2003; Luu et al., 2001; Song et al., 2015), it remains unclear how imperfect spatial sampling influences source imaging (Michel and He, 2011). It is noteworthy that even when 32 channels are used, as was done in the present study, source localization can provide useful insight into underlying brain activity (Ding et al., 2006, 2007; Sperli et al., 2006; Zhang et al., 2003). Despite the challenge of the EEG inverse problem, valid solution estimates are feasible if reasonable constraints are placed on the equivalent source distribution (Pascual-Marqui et al., 1994). For example, because brain EEG sources are assumed to consist of a few moving equivalent current dipoles (He et al., 1987), we estimated a solution to the EEG inverse problem in accordance with other findings in clinical neurophysiology. Nevertheless, both CFC and Granger causality analyses can be improved upon for the better investigation of functional causal connectivity. This should be carefully factored into the interpretation of our present observations. With regard to the current findings in the sensor space, although the electrodes Fz and Cz were located in close proximity to one another, we observed one-way directional causality between these electrodes (i.e., delta-phase/high-gamma-amplitude coupling for the Fz-phase/Cz-amplitude combination, but not for the Cz-phase/Fz-amplitude combination; Fig. 2A). Regarding the functional dissociation between activity at the Fz and Cz electrodes, our previous study (Hong et al., 2016) consistently showed that in the ERP scalp topographical distributions; the most dominant activity was centered around Cz during the processing of target stimuli, whereas it was centered around Fz during the processing of standard stimuli. Although these different ERP dynamics were driven by auditory stimuli, the findings are an example of functional dissociation between activity at Fz and Cz and suggest that EEG dynamics at Fz may be independent from those at Cz in the resting state. Second, although a larger sample size would have improved the statistical power of our study, sample sizes were limited by patient subgrouping. Despite the use of non-parametric statistical tests (e.g., Mann-Whitney *U* test), the limited statistical power should be carefully considered when interpreting our *post hoc* comparisons between the T1 and T2 groups. Third, audiograms in the present study were measured up to 8 kHz. Although the extension to higher frequencies over 8 kHz may have improved the ability of our hearing assessments to detect hidden hearing loss, the clinical significance of such high-frequency hearing tests is still unclear (Balatsouras et al., 2005; Osterhammel and Osterhammel, 1979; Schmuziger et al., 2007). Indeed, hidden hearing loss refers to all frequencies that are not tested by routine audiometry. Hidden hearing loss can equally be within not only higher but also lower frequencies of the measured range; therefore, detecting such loss would require the use of high-resolution audiometry or ABRs. As such, the definition of normal hearing in the present study should be carefully considered as possibly including hidden hearing loss. Fourth, in the present study, the resting-state EEG signals were recorded for 5 min. Previous functional magnetic resonance imaging (fMRI) studies have suggested that longer scans (at least 12 min) may be more reliable (Birn et al., 2013; Laumann et al., 2015; Pannunzi et al., 2017). However, this may be different for EEG/MEG-based functional connectivity. Using only 4-min scans, Kuntzelman and Miskovic (2017) showed that the reliability of EEG connectivity varies depending on the frequency band. Nevertheless, their study suffered from the same errors associated with previous fMRI resting-state studies, that is, the lack of longer-duration measurements. Thus, our 5-min recordings should be carefully considered when interpreting the current observations; additional studies that utilize longer EEG-recording periods should be performed to confirm our findings. Lastly, since only patients with tinnitus without hearing loss participated in the present study, further experiments on tinnitus with hearing loss are necessary to confirm a lack of resting-state delta-phase/gamma-amplitude coupling in patients with tinnitus compared to healthy participants. A future study using the same experimental paradigm

to evaluate patients with tinnitus and hearing loss will provide more information about the neural signature of tinnitus in the resting state.

5. Conclusions

Abnormal low-frequency connectivity together with the absence of delta/high-gamma PAC in patients with tinnitus may reflect impaired prefrontal top-down inhibitory control and deficient integration and communication over inter-regional functional brain networks in the resting state. Our observations are indicative of maladaptive neuroplasticity or abnormal reorganization in the auditory default mode network in tinnitus. Moreover, delta/high-gamma PAC may be a reliable biomarker for tinnitus symptoms, even in the resting state.

Acknowledgements

This work was supported by the Basic Science Research program (grant numbers 2015R1A1A1A05027233 to BKM; 2017M3A9G1027932 to SKH), the ICT R&D program of MSIP/Institute for Information & Communications Technology Promotion (IITP; grant number 2017-0-00432 to BKM), and the Information Technology Research Center (ITRC) support program (grant number IITP-2017-2016-0-00464 to BKM) supervised by the IITP, which are funded by the Korean government (MSIT) through the National Research Foundation of Korea. The authors declare that they have no competing interests.

Appendix A. Supplementary data

Supplementary data related to this article can be found at https://doi.org/10.1016/j.heares.2017.10.008.

References

Adamchic, I., Langguth, B., Hauptmann, C., Tass, P.A., 2014. Abnormal cross-frequency coupling in the tinnitus network. Front. Neurosci. 8, 284.
Adjamian, P., Sereda, M., Zobay, O., Hall, D.A., Palmer, A.R., 2012. Neuromagnetic indicators of tinnitus and tinnitus masking in patients with and without hearing loss. J. Assoc. Res. Otolaryngol. 13, 715–731.
Alain, C., Woods, D.L., Knight, R.T., 1998. A distributed cortical network for auditory sensory memory in humans. Brain Res. 812, 23–37.
Apps, M.A., Balsters, J.H., Ramnani, N., 2012. The anterior cingulate cortex: monitoring the outcomes of others' decisions. Soc. Neurosci. 7, 424–435.
Astolfi, L., Cincotti, F., Mattia, D., Salinari, S., Babiloni, C., Basilisco, A., Rossini, P.M., Ding, L., Ni, Y., He, B., Marciani, M.G., Babiloni, F., 2004. Estimation of the effective and functional human cortical connectivity with structural equation modeling and directed transfer function applied to high-resolution EEG. Magn. Reson. Imaging 22, 1457–1470.
Astolfi, L., Cincotti, F., Mattia, D., Marciani, M.G., Baccala, L.A., Fallani, F.D., Salinari, S., Ursino, M., Zavaglia, M., Ding, L., Edgar, J.C., Miller, G.A., He, B., Babiloni, F., 2007. Comparison of different cortical connectivity estimators for high-resolution EEG recordings. Hum. Brain Mapp. 28, 143–157.
Babiloni, F., Cincotti, F., Babiloni, C., Carducci, F., Mattia, D., Astolfi, L., Basilisco, A., Rossini, P.M., Ding, L., Ni, Y., Cheng, J., Christine, K., Sweeney, J., He, B., 2005. Estimation of the cortical functional connectivity with the multimodal integration of high-resolution EEG and fMRI data by directed transfer function. NeuroImage 24, 118–131.
Balatsouras, D.G., Homsioglou, E., Danielidis, V., 2005. Extended high-frequency audiometry in patients with acoustic trauma. Clin. Otolaryngol. 30, 249–254.
Benchenane, K., Peyrache, A., Khamassi, M., Tierney, P.L., Gioanni, Y., Battaglia, F.P., Wiener, S.I., 2010. Coherent theta oscillations and reorganization of spike timing in the hippocampal-prefrontal network upon learning. Neuron 66, 921–936.
Birn, R.M., Molloy, E.K., Patriat, R., Parker, T., Meier, T.B., Kirk, G.R., Nair, V.A., Meyerand, M.E., Prabhakaran, V., 2013. The effect of scan length on the reliability of resting-state fMRI connectivity estimates. NeuroImage 83, 550–558.
Borsa, V.M., Della Rosa, P.A., Catricala, E., Canini, M., Iadanza, A., Falini, A., Abutalebi, J., Iannaccone, S., 2016. Interference and conflict monitoring in individuals with amnestic mild cognitive impairment: a structural study of the anterior cingulate cortex. J. Neuropsychol. https://doi.org/10.1111/jnp.12105.
Botvinick, M.M., Cohen, J.D., Carter, C.S., 2004. Conflict monitoring and anterior cingulate cortex: an update. Trends Cogn. Sci. 8, 539–546.
Buzsaki, G., Draguhn, A., 2004. Neuronal oscillations in cortical networks. Science 304, 1926–1929.
Canolty, R.T., Knight, R.T., 2010. The functional role of cross-frequency coupling. Trends Cogn. Sci. 14, 506–515.
Canolty, R.T., Edwards, E., Dalal, S.S., Soltani, M., Nagarajan, S.S., Kirsch, H.E., Berger, M.S., Barbaro, N.M., Knight, R.T., 2006. High gamma power is phase-locked to theta oscillations in human neocortex. Science 313, 1626–1628.
Caporello Bluvas, E., Gentner, T.Q., 2013. Attention to natural auditory signals. Hear. Res. 305, 10–18.
Carpenter-Thompson, J.R., Schmidt, S.A., Husain, F.T., 2015. Neural plasticity of mild tinnitus: an fMRI investigation comparing those recently diagnosed with tinnitus to those that had tinnitus for a long period of time. Neural Plast. 2015, 161478.
Cohen, M.X., 2008. Assessing transient cross-frequency coupling in EEG data. J. Neurosci. Methods 168, 494–499.
Dai, Y., He, B., 2011. MEG-based brain functional connectivity analysis using eConnectome. In: The 8th International Symposium on Noninvasive Functional Source Imaging of the Brain and Heart & the 8th International Conference on Bioelectromagnetism (NFSI & ICBEM). IEEE, pp. 9–11.
Dai, Y., Zhang, W., Dickens, D.L., He, B., 2012. Source connectivity analysis from MEG and its application to epilepsy source localization. Brain Topogr. 25, 157–166.
Dale, A.M., Sereno, M.I., 1993. Improved localizadon of cortical activity by combining EEG and MEG with MRI cortical surface reconstruction: a linear approach. J. Cogn. Neurosci. 5, 162–176.
Darvas, F., Ermer, J.J., Mosher, J.C., Leahy, R.M., 2006. Generic head models for atlas-based EEG source analysis. Hum. Brain Mapp. 27, 129–143.
Ding, L., Worrell, G.A., Lagerlund, T.D., He, B., 2006. 3D source localization of interictal spikes in epilepsy patients with MRI lesions. Phys. Med. Biol. 51, 4047–4062.
Ding, L., Worrell, G.A., Lagerlund, T.D., He, B., 2007. Ictal source analysis: localization and imaging of causal interactions in humans. NeuroImage 34, 575–586.
Donchin, E., Coles, M.G.H., 1988. Is the P300 component a manifestation of context updating? Behav. Brain Sci. 11, 357–427.
Faber, M., Vanneste, S., Fregni, F., De Ridder, D., 2012. Top down prefrontal affective modulation of tinnitus with multiple sessions of tDCS of dorsolateral prefrontal cortex. Brain Stimul. 5, 492–498.
Fletcher, P.C., Frith, C.D., Grasby, P.M., Shallice, T., Frackowiak, R.S.J., Dolan, R.J., 1995. Brain systems for encoding and retrieval of auditory–verbal memory. An in vivo study in humans. Brain 118, 401–416.
Fuster, J.M., 1989. The Prefrontal Cortex: Anatomy, Physiology, and Neuropsychology of the Frontal Lobe, second ed. Raven Press, New York.
Fuster, J.M., 2008. The Prefrontal Cortex, fourth ed. Academic Press, Cambridge.
Fuster, J.M., 2013. Cognitive functions of the prefrontal cortex. In: Stuss, D.T., Knight, R.T. (Eds.), Principles of Frontal Lobe Function, second ed. Oxford University Press, New York, pp. 11–22.
Gazzaley, A., D'Esposito, M., 2007. Unifying prefrontal cortex function: executive control, neural networks, and top-down modulation. In: Miller, B.L., Cummings, J.L. (Eds.), The Human Frontal Lobes: Functions and Disorders, second ed. The Guilford Press, New York, pp. 187–206.
Goncharova, I.I., McFarland, D.J., Vaughan, T.M., Wolpaw, J.R., 2003. EMG contamination of EEG: spectral and topographical characteristics. Clin. Neurophysiol. 114, 1580–1593.
Granger, C.W.J., 1969. Investigating causal relations by econometric models and cross-spectral methods. Econometrica 37, 424–438.
He, B., Musha, T., Okamoto, Y., Homma, S., Nakajima, Y., Sato, T., 1987. Electric dipole tracing in the brain by means of the boundary element method and its accuracy. IEEE Trans. Bio-Med. Eng. 34, 406–414.
He, B., Dai, Y.K., Astolfi, L., Babiloni, F., Yuan, H., Yang, L., 2011. eConnectome: a MATLAB toolbox for mapping and imaging of brain functional connectivity. J. Neurosci. Methods 195, 261–269.
Heeren, A., Maurage, P., Perrot, H., De Volder, A., Renier, L., Araneda, R., Lacroix, E., Decat, M., Deggouj, N., Philippot, P., 2014. Tinnitus specifically alters the top-down executive control sub-component of attention: evidence from the attention network task. Behav. Brain Res. 269, 147–154.
Hong, S.K., Park, S., Ahn, M.H., Min, B.K., 2016. Top-down and bottom-up neurodynamic evidence in patients with tinnitus. Hear. Res. 342, 86–100.
Jastreboff, P.J., Sasaki, C.T., 1994. An animal model of tinnitus: a decade of development. Am. J. Otol. 15, 19–27.
Johnson, R., 1988. The amplitude of the P300 component of the event-related potential: review and synthesis. Adv. Psychophysiol. 3, 69–137.
Johnston, K., Levin, H.M., Koval, M.J., Everling, S., 2007. Top-down control-signal dynamics in anterior cingulate and prefrontal cortex neurons following task switching. Neuron 53, 453–462.
Kaya, E.M., Elhilali, M., 2014. Investigating bottom-up auditory attention. Front. Hum. Neurosci. 8, 327.
Keeser, D., Padberg, F., Reisinger, E., Pogarell, O., Kirsch, V., Palm, U., Karch, S., Moller, H.J., Nitsche, M.A., Mulert, C., 2011. Prefrontal direct current stimulation modulates resting EEG and event-related potentials in healthy subjects: a standardized low resolution tomography (sLORETA) study. NeuroImage 55, 644–657.
Kemp, D.T., 1978. Stimulated acoustic emissions from within human auditory-system. J. Acoust. Soc. Am. 64, 1386–1391.
Klem, G.H., 2003. Artifacts. In: Ebersole, J.S., Pedley, T.A. (Eds.), Current Practice of Clinical Electroencephalography. Lippincott Williams & Wilkins, Philadelphia, pp. 271–287.

Kujawa, S.G., Liberman, M.C., 2009. Adding insult to injury: cochlear nerve degeneration after “temporary” noise-induced hearing loss. J. Neurosci. 29, 14077–14085.
Kuntzelman, K., Miskovic, V., 2017. Reliability of graph metrics derived from resting-state human EEG. Psychophysiology 54, 51–61.
Lakatos, P., Shah, A.S., Knuth, K.H., Ulbert, I., Karmos, G., Schroeder, C.E., 2005. An oscillatory hierarchy controlling neuronal excitability and stimulus processing in the auditory cortex. J. Neurophysiol. 94, 1904–1911.
Lantz, G., de Peralta, R.G., Spinelli, L., Seeck, M., Michel, C.M., 2003. Epileptic source localization with high density EEG: how many electrodes are needed? Clin. Neurophysiol. 114, 63–69.
Laumann, T.O., Gordon, E.M., Adeyemo, B., Snyder, A.Z., Joo, S.J., Chen, M.Y., Gilmore, A.W., McDermott, K.B., Nelson, S.M., Dosenbach, N.U.F., Schlaggar, B.L., Mumford, J.A., Poldrack, R.A., Petersen, S.E., 2015. Functional system and areal organization of a highly sampled individual human brain. Neuron 87, 657–670.
Legatt, A.D., 2011. Intraoperative evoked potential monitoring. In: Schomer, D.L., Lopes da Silva, F.H. (Eds.), Electroencephalography: Basic Principles, Clinical Applications, and Related Fields, sixth ed. Lippincott Williams & Wilkins, Philadelphia, pp. 767–786.
Lewis, J.W., Beauchamp, M.S., DeYoe, E.A., 2000. A comparison of visual and auditory motion processing in human cerebral cortex. Cereb. Cortex 10, 873–888.
Li, F., Liu, T., Wang, F., Li, H., Gong, D., Zhang, R., Jiang, Y., Tian, Y., Guo, D., Yao, D., Xu, P., 2015. Relationships between the resting-state network and the P3: evidence from a scalp EEG study. Sci. Rep. 5, 15129.
Lisman, J., 2005. The theta/gamma discrete phase code occurring during the hippocampal phase precession may be a more general brain coding scheme. Hippocampus 15, 913–922.
Lisman, J.E., Idiart, M.A.P., 1995. Storage of 7+/-2 short-term memories in oscillatory subcycles. Science 267, 1512–1515.
Llinas, R.R., Ribary, U., Jeanmonod, D., Kronberg, E., Mitra, P.P., 1999. Thalamocortical dysrhythmia: a neurological and neuropsychiatric syndrome characterized by magnetoencephalography. Proc. Natl. Acad. Sci. 96, 15222–15227.
Luo, H., Poeppel, D., 2007. Phase patterns of neuronal responses reliably discriminate speech in human auditory cortex. Neuron 54, 1001–1010.
Luu, P., Tucker, D.M., Englander, R., Lockfeld, A., Lutsep, H., Oken, B., 2001. Localizing acute stroke-related EEG changes: assessing the effects of spatial undersampling. J. Clin. Neurophysiol. 18, 302–317.
Makeig, S., Jung, T.P., Bell, A.J., Ghahremani, D., Sejnowski, T.J., 1997. Blind separation of auditory event-related brain responses into independent components. Proc. Natl. Acad. Sci. 94, 10979–10984.
McNamee, D., Liljeholm, M., Zika, O., O'Doherty, J.P., 2015. Characterizing the associative content of brain structures involved in habitual and goal-directed actions in humans: a multivariate fMRI study. J. Neurosci. 35, 3764–3771.
Michel, C.M., He, B., 2011. EEG mapping and source imaging. In: Schomer, D.L., Lopes da Silva, F.H. (Eds.), Electroencephalography: Basic Principles, Clinical Applications, and Related Fields, sixth ed. Lippincott Williams & Wilkins, Philadelphia, pp. 1179–1202.
Miller, B.L., Cummings, J.L., 2007. The Human Frontal Lobes: Functions and Disorders, second ed. Guilford Press, New York.
Miller, R., 2013. Cortico-hippocampal Interplay and the Representation of Contexts in the Brain. Springer Science & Business Media, Berlin.
Mills, D.M., Rubel, E.W., 1994. Variation of distortion-product otoacoustic emissions with furosemide injection. Hear. Res. 77, 183–199.
Min, B.K., Park, H.J., 2010. Task-related modulation of anterior theta and posterior alpha EEG reflects top-down preparation. BMC Neurosci. 11, 79.
Mitchell, T.V., Morey, R.A., Inan, S., Belger, A., 2005. Functional magnetic resonance imaging measure of automatic and controlled auditory processing. Neuroreport 16, 457–461.
Mohamad, N., Hoare, D.J., Hall, D.A., 2016. The consequences of tinnitus and tinnitus severity on cognition: a review of the behavioural evidence. Hear. Res. 332, 199–209.
Moller, A.R., Jannetta, P.J., 1982. Evoked potentials from the inferior colliculus in man. Electroencephalogr. Clin. Neurophysiol. 53, 612–620.
Moller, A.R., Jannetta, P., Bennett, M., Moller, M.B., 1981. Intracranially recorded responses from the human auditory nerve: new insights into the origin of brain stem evoked potentials (BSEPs). Electroencephalogr. Clin. Neurophysiol. 52, 18–27.
Muhlau, M., Rauschecker, J.P., Oestreicher, E., Gaser, C., Rottinger, M., Wohlschlager, A.M., Simon, F., Etgen, T., Conrad, B., Sander, D., 2006. Structural brain changes in tinnitus. Cereb. Cortex 16, 1283–1288.
Muthukumaraswamy, S.D., 2013. High-frequency brain activity and muscle artifacts in MEG/EEG: a review and recommendations. Front. Hum. Neurosci. 7, 138.
Näätänen, R., Teder, W., Alho, K., Lavikainen, J., 1992. Auditory attention and selective input modulation - a Topographical ERP Study. Neuroreport 3, 493–496.
Newman, C.W., Jacobson, G.P., Spitzer, J.B., 1996. Development of the tinnitus handicap inventory. Arch. Otolaryngol. Head Neck Surg. 122, 143–148.
Norena, A., Cransac, H., Chery-Croze, S., 1999. Towards an objectification by classification of tinnitus. Clin. Neurophysiol. 110, 666–675.
Osipova, D., Hermes, D., Jensen, O., 2008. Gamma power is phase-locked to posterior alpha activity. PLoS ONE 3, e3990.
Osterhammel, D., Osterhammel, P., 1979. High-frequency audiometry: age and sex variations. Scand. Audiol. 8, 73–80.
Pannunzi, M., Hindriks, R., Bettinardi, R.G., Wenger, E., Lisofsky, N., Martensson, J., Butler, O., Filevich, E., Becker, M., Lochstet, M., Kühn, S., Deco, G., 2017. Resting-state fMRI correlations: from link-wise unreliability to whole brain stability. NeuroImage 157, 250–262.
Pascual-Marqui, R.D., Michel, C.M., Lehmann, D., 1994. Low resolution electromagnetic tomography: a new method for localizing electrical activity in the brain. Int. J. Psychophysiol. 18, 49–65.
Picton, T.W., 1992. The P300 wave of the human event-related potential. J. Clin. Neurophysiol. 9, 456–479.
Pierzycki, R.H., McNamara, A.J., Hoare, D.J., Hall, D.A., 2016. Whole scalp resting state EEG of oscillatory brain activity shows no parametric relationship with psychoacoustic and psychosocial assessment of tinnitus: a repeated measures study. Hear. Res. 331, 101–108.
Polich, J., 1993. Cognitive brain potentials. Curr. Dir. Psychol. Sci. 2, 175–179.
Rizzuto, D.S., Madsen, J.R., Bromfield, E.B., Schulze-Bonhage, A., Kahana, M.J., 2006. Human neocortical oscillations exhibit theta phase differences between encoding and retrieval. NeuroImage 31, 1352–1358.
Roberts, L.E., Husain, F.T., Eggermont, J.J., 2013. Role of attention in the generation and modulation of tinnitus. Neurosci. Biobehav. Rev. 37, 1754–1773.
Saleh, M., Reimer, J., Penn, R., Ojakangas, C.L., Hatsopoulos, N.G., 2010. Fast and slow oscillations in human primary motor cortex predict oncoming behaviorally relevant cues. Neuron 65, 461–471.
Schaette, R., McAlpine, D., 2011. Tinnitus with a normal audiogram: physiological evidence for hidden hearing loss and computational model. J. Neurosci. 31, 13452–13457.
Schlee, W., Weisz, N., Bertrand, O., Hartmann, T., Elbert, T., 2008. Using auditory steady state responses to outline the functional connectivity in the tinnitus brain. PLoS ONE 3, e3720.
Schlee, W., Hartmann, T., Langguth, B., Weisz, N., 2009a. Abnormal resting-state cortical coupling in chronic tinnitus. BMC Neurosci. 10, 11.
Schlee, W., Mueller, N., Hartmann, T., Keil, J., Lorenz, I., Weisz, N., 2009b. Mapping cortical hubs in tinnitus. BMC Biol. 7, 80.
Schmuziger, N., Patscheke, J., Probst, R., 2007. An assessment of threshold shifts in nonprofessional pop/rock musicians using conventional and extended high-frequency audiometry. Ear Hear. 28, 643–648.
Schroeder, C.E., Lakatos, P., 2009. Low-frequency neuronal oscillations as instruments of sensory selection. Trends Neurosci. 32, 9–18.
Schutter, D.J.L.G., Knyazev, G.G., 2012. Cross-frequency coupling of brain oscillations in studying motivation and emotion. Motiv. Emot. 36, 46–54.
Silton, R.L., Heller, W., Towers, D.N., Engels, A.S., Spielberg, J.M., Edgar, J.C., Sass, S.M., Stewart, J.L., Sutton, B.P., Banich, M.T., Miller, G.A., 2010. The time course of activity in dorsolateral prefrontal cortex and anterior cingulate cortex during top-down attentional control. NeuroImage 50, 1292–1302.
Song, J., Davey, C., Poulsen, C., Luu, P., Turovets, S., Anderson, E., Li, K., Tucker, D., 2015. EEG source localization: sensor density and head surface coverage. J. Neurosci. Methods 256, 9–21.
Sperli, F., Spinelli, L., Seeck, M., Kurian, M., Michel, C.M., Lantz, G., 2006. EEG source imaging in pediatric epilepsy surgery: a new perspective in presurgical workup. Epilepsia 47, 981–990.
Squire, L.R., Ojemann, J.G., Miezin, F.M., Petersen, S.E., Videen, T.O., Raichle, M.E., 1992. Activation of the hippocampus in normal humans: a functional anatomical study of memory. Proc. Natl. Acad. Sci. 89, 1837–1841.
Srinivasan, R., Tucker, D.M., Murias, M., 1998. Estimating the spatial Nyquist of the human EEG. Behav. Res. Methods, Instrum. Comput. 30, 8–19.
Tadel, F., Baillet, S., Mosher, J.C., Pantazis, D., Leahy, R.M., 2011. Brainstorm: a user-friendly application for MEG/EEG analysis. Comput. Intell. Neurosci. 2011, 879716.
Teki, S., Kumar, S., von Kriegstein, K., Stewart, L., Lyness, C.R., Moore, B.C.J., Capleton, B., Griffiths, T.D., 2012. Navigating the auditory scene: an expert role for the hippocampus. J. Neurosci. 32, 12251–12257.
Tort, A.B.L., Komorowski, R., Eichenbaum, H., Kopell, N., 2010. Measuring phase-amplitude coupling between neuronal oscillations of different frequencies. J. Neurophysiol. 104, 1195–1210.
Valdes-Hernandez, P.A., von Ellenrieder, N., Ojeda-Gonzalez, A., Kochen, S., Aleman-Gomez, Y., Muravchik, C., Valdes-Sosa, P.A., 2009. Approximate average head models for EEG source imaging. J. Neurosci. Methods 185, 125–132.
Van Dijk, K.R.A., Hedden, T., Venkataraman, A., Evans, K.C., Lazar, S.W., Buckner, R.L., 2010. Intrinsic functional connectivity as a tool for human connectomics: theory, properties, and optimization. J. Neurophysiol. 103, 297–321.
Vanneste, S., Joos, K., De Ridder, D., 2012. Prefrontal cortex based sex differences in tinnitus perception: same tinnitus intensity, same tinnitus distress, different mood. PLoS ONE 7, e31182.
Vanneste, S., Plazier, M., der Loo, E., de Heyning, P.V., Congedo, M., De Ridder, D., 2010. The neural correlates of tinnitus-related distress. NeuroImage 52, 470–480.
Vertes, R.P., 2005. Hippocampal theta rhythm: a tag for short-term memory. Hippocampus 15, 923–935.
Voisin, J., Bidet-Caulet, A., Bertrand, O., Fonlupt, P., 2006. Listening in silence activates auditory areas: a functional magnetic resonance imaging study. J. Neurosci. 26, 273–278.
von Stein, A., Sarnthein, J., 2000. Different frequencies for different scales of cortical integration: from local gamma to long range alpha/theta synchronization. Int. J.

Psychophysiol. 38, 301–313.
Voytek, B., Canolty, R.T., Shestyuk, A., Crone, N.E., Parvizi, J., Knight, R.T., 2010. Shifts in gamma phase-amplitude coupling frequency from theta to alpha over posterior cortex during visual tasks. Front. Hum. Neurosci. 4, 191.
Weisz, N., Hartmann, T., Dohrmann, K., Schlee, W., Norena, A., 2006. High-frequency tinnitus without hearing loss does not mean absence of deafferentation. Hear. Res. 222, 108–114.
World Medical Association, 2013. World Medical Association declaration of Helsinki: ethical principles for medical research involving human subjects. JAMA 310, 2191–2194.
Zhang, X., van Drongelen, W., Hecox, K.E., Towle, V.L., Frim, D.M., McGee, A.B., He, B., 2003. High-resolution EEG: cortical potential imaging of interictal spikes. Clin. Neurophysiol. 114, 1963–1973.